TOUCHLESS-TO-TOUCH FINGERPRINT SYSTEMS COMPATIBILITY METHOD

P. Salum, D. Sandoval *

Loop Computer Engineering
Brasília, Brazil

A. Zaghetto, B. Macchiavello, C. Zaghetto†

University of Brasília
Department of Computer Science
Brasília, Brazil

ABSTRACT

Touchless multiview fingerprinting technology has been proposed as an alternative to overcome intrinsic problems of traditional touchbased systems. However, if one wants to benefit from the advantages presented by touchless scanners, the captured images must be processed in order to become compatible to touchbased systems. This paper proposes a two-step solution to the touchless-to-touch compatibility problem. First, it reproduces the texture of touchbased acquisition; and second, it performs a geometric transformation in order to approximate the nail-to-nail touchbased enrollment process. Two experiments were proposed, one to evaluate the quality of the processed images, another one to estimate the EER (equal error rate) for a set of 200 fingerprints (100 fingers, 2 images per finger). Results show that 90% of the images presented good, very good or excellent scores according to NFIQ. In addition, the observed EER was approximately 4%, demonstrating the viability of the proposed method.

1. INTRODUCTION

Biometric authentication can be defined as the automatic recognition of an individual using physiological or behavioral characteristics [1]. Fingerprints, hand geometry, voice, iris, face and keystroke dynamics are examples of such characteristics. In general, different biometrics require different technologies. However, regardless of the particularities concerning a specific biometric, there are common issues that affect most of them, such as the interoperability between devices and systems. It is not easy to determine which biometric feature is the most appropriate. This decision depends on the applications and operating conditions in which the systems operate. Nevertheless, fingerprints are one of the most popular in forensics, civilian and commercial applications [2].

In general, fingerprint technologies deal with touchbased acquisitions. That means they require users to press their fingers against an acquisition surface. However, solutions that do not demand contact (touchless) are increasingly being proposed [3, 4, 5, 6, 7] in order to overcome the intrinsic problems related to touchbased technologies. Despite the advantages of the touchless approach and considering that touchbased systems are still broadly used, the interoperability between these two paradigms is mandatory if one wants to benefit from the new features that touchless systems offer. Therefore, the main objective in this paper is to present a method that enables compatibility between touchbased and touchless fingerprint systems. Next, these two paradigms are discussed, as well as the compatibility problem.

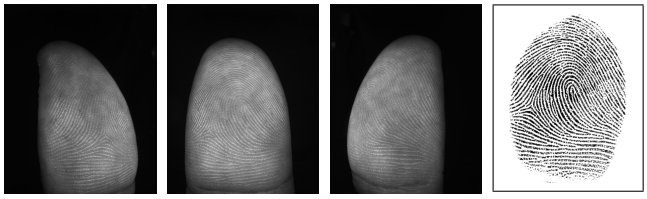

(a) View 2 (b) View 0 (c) View 1 (d) touch

Fig. 1. Comparison between touchless and touchbased fingerprints: (a), (b) and (c) examples of views captured by a touchless multiview fingerprint scanner (1024×1280 pixels, 8 bits/pixels); and (d) an example of a touchbased scan of the same finger equivalent to View 0.

1.1. Touchbased Fingerprints

The biggest problem that arises from touchbased fingerprints are distortions and inconsistencies that may be introduced due to the elasticity of the skin. The quality of fingerprints can also be seriously affected by the non-ideal contact caused by dirt, sweat, moisture, excessive dryness or humidity, temperature and latent fingerprints. Furthermore, different parts of the same finger may be captured each time it is presented to the sensor, resulting in irreproducible samples. In some scenarios such disadvantages may demand the need of a trained operator during the registration phase and, in many cases, multiple acquisition attempts of the same finger are executed until samples with sufficient quality are produced. Although some algorithms have been proposed in order to compensate the limitations of touchbased systems, this paradigm may represent a bottleneck regarding the quality of acquired fingerprint

*E-mails: {pedro, daniel}@loopce.com.
†E-mails: {zaghetto, bruno}@unb.br, zaghettoc@bitgroup.co.
This work was partially supported by CNPq under grant 307737/2015-2.

images.

1.2. Touchless Fingerprints

Touchless fingerprinting addresses the problem of quality at its fundamental level, which is the way fingerprint images are captured. Since it does not require the user to press his fingers on a surface, such systems do not need, for example, algorithms that compensate artifacts resulting from skin elasticity or non-ideal contact. Among the touchless solutions, the devices developed by TBS (Touchless Biometrics System)[1] uses a very interesting approach [7]. It is based on a three-camera multiview acquisition system. One camera (View 0) is positioned in such a way it captures the part of the finger where cores and deltas are usually located and, using this camera as reference, two other cameras are positioned at 45 degrees clockwise (View 2) and at 45 degrees counterclockwise (View 1). Since the overlap of their fields of view is assured, it is possible to capture a large area and generate touchless nail-to-nail fingerprint using a stitching algorithm [8]. Figures 1(a)-(c) show an example of three views captured by a multiview touchless device.

1.3. Compatibility

In general, images captured by touchless technologies are not compatible to those obtained by traditional touchbased scanners, particularly to those in which the nail-to-nail rolling of the fingers on a flat, transparent and backlit surface is required. For comparison, Fig. 1(d) shows a touchbased acquisition equivalent to View 0. One should notice the clear difference between the textures of both finger representations.

In order to take advantage of the operational benefits offered by touchless scanners (less elastic distortion, faster acquisition, increased usability, hygiene, acceptability, etc.) [6], images captured by these devices need to be processed in order to become similar to those acquired using conventional touchbased scanners. Next, a solution to the compatibility problem is proposed.

2. PROPOSED METHOD

Figure 2 presents a block diagram that summarizes the proposed method. The initial steps consist of classical image enhancement techniques. The input image I, which is acquired by a multiview touchless device, represents the stitched version of all views shown in Figs. 1(a)-(c). The result is shown in Fig. 3(a).

First, a local histogram equalization is performed using blocks of 8×8 pixels. This generates an equalized image I_h. The next step is a gamma transformation, defined by Eq. 1,

$$I_{h\gamma} = c \cdot I_h^{\gamma}, \tag{1}$$

[1] http://www.tbsinc.com/

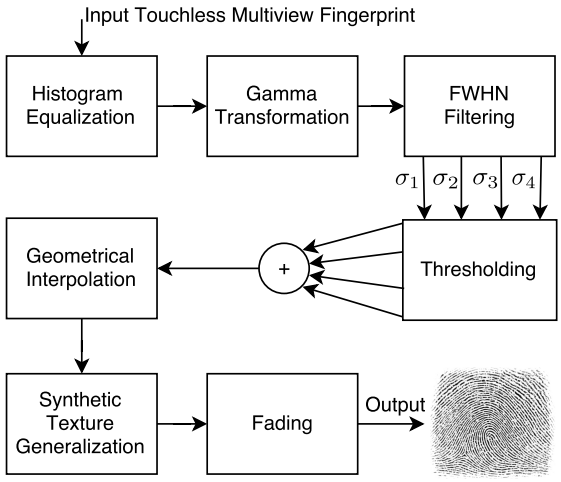

Fig. 2. Block Diagram of the proposed method.

where γ determines the contrast enhancement itself, while c is used for normalization. Both c and γ parameters are positive. During the implementation of the proposed method, and after empirical tests, these constants were set to $c = 0.25$ and $\gamma = 1.5$. The resulting image, $I_{h\gamma}$, obtained after local histogram equalization is presented in Fig. 3(b).

Next, low-pass Gaussian filtering is performed. In fact, four different filters are used, each one with a different kernel size $h_i = [3\ 5\ 7\ 9]$. Since the filters used are full width at half maximum filters (FWHM), standard deviation values σ_i are obtained as a function of h_i, as defined in Eq. 2. The reason for using four different filters is that each one may capture different aspects of the fingerprint. The idea is to emphasize what is similar, rather than what is different. The four resulting images are later used to compose a single binary image and the most common characteristics to all of them will be more relevant than specific artifacts.

$$\sigma_i = \frac{h_i}{2\sqrt{2\ln 2}}. \tag{2}$$

The four images resulting from the filtering process, referred to as I_{fi} ($i = 1..4$) are binarized by the $mindtct$ software, which is a tool developed by the National Institute of Standards and Technology (NIST) and included in the NIST Biometric Image Software (NBIS) [9] package. It is meant to detect minutiae, but as an intermediate step a binarized version of the input fingerprint is generated. Figures 3(c) and (d) show I_{f1}, the result of the filtering process for $h_1 = 3$, and I_{b1}, its binarized version. For the sake of briefness, the images I_{fi} and I_{bi}, for $i = 2..4$ are not presented.

Then, a single image I_M is generated from the average of I_{bi} ($i = 1..4$). An example is presented in Fig. 4(a), which shows a fingerprint that starts to look similar to those acquired by a conventional touchbased scanner. However, there are still two significant differences: the texture and the acquisition geometry of the acquired area.

From Fig. 4(a) one may notice that the bottommost row of the fingerprint is wider then the uppermost row. Usually an image acquired using a conventional device in which the finger is rolled from nail-to-nail does not have this so pronounced asymmetrical aspect. Therefore, a geometrical correction of the upper part of the image is required. The proposed method initially estimates the left and right contours of I_M using a 5th-degree polynomial regression. It is assumed that these contours are vertically symmetrical, which means once a polynomial that describes the left contour, p_{left}, is found, then we can use a symmetric polynomial, p_{right}, for the estimation of the right contour. Once estimated, the polynomials are used to perform a bicubic interpolation at each row, separately. The objective is to make the length of all fingerprint rows as close as possible to the length of the bottom most row. Figure 4(b) shows an example of fingerprint image I_D that results from the described geometrical correction.

To solve the problem of texture, we use part of a known method that generates synthetic fingerprints [10]. Here the intent is just to add texture to the processed fingerprint, instead of synthesizing an entire image. Therefore, different ellipses are added to I_D, with positions, major axis (between 1 and 5 pixels), minor axis (between 1 and 3 pixel), angles (between 0 and 180°) and luminance values (between 0 and 255) randomly chosen. The result, I_T, is illustrated in Fig. 4 (c).

Finally, due to the nature of touchless devices, and the effects of binarization, Gaussian filtering and geometrical correction, the contours of the fingers do not appear natural. In order eliminate this artificial aspect, a fading process is applied. The left and the right contours are horizontally faded according to quadratic functions, thus preserving some of the original curvature of I_T. Top and bottom parts are vertically faded along horizontal lines. Fading is first applied horizontally and then vertically. If $I_T(i,j)$ represents a pixel at position (i,j), then its horizontally faded version is obtained by $I_F(i,j) = I_T(i,j) + \Delta(d_h)$, where $\Delta(d_h)$ is a gray level between 0 and 255. The value of $\Delta(d_h)$ is proportional to the horizontal distance d_h between the point located at the quadratic function that represents the new parabolic vertical limit of the fingerprint and any column j. If the pixel is near these contours, the value of $\Delta(d_h)$ is close to 0 and increases along the horizontal distance. As for the vertical fading, the process is analogous. In this case, the adding factor is changed from $\Delta(d_h)$ to $\Delta(d_v)$, where d_v represents the vertical distance between the top or bottom horizontal limits any row i. The factor $\Delta(d_v)$ also increases with distance. Only pixels that are outside the limits are processed. Finally, I_F is cropped to a maximum value of 255. The final image is presented in Fig. 4(d).

3. EXPERIMENTAL RESULTS

In our experiments the test set consists of 200 images acquired by a touchless multiview fingerprint device. The fingerprints were captured in the most natural way, simulating the operating conditions of a real autonomous acquisition process. In other words, the influence of an operator was as much as possible minimized. His participation was limited to indicate the moment at which the user should position the finger into the device. Moreover, no image was discarded. Even those that could be classified as of poor quality.

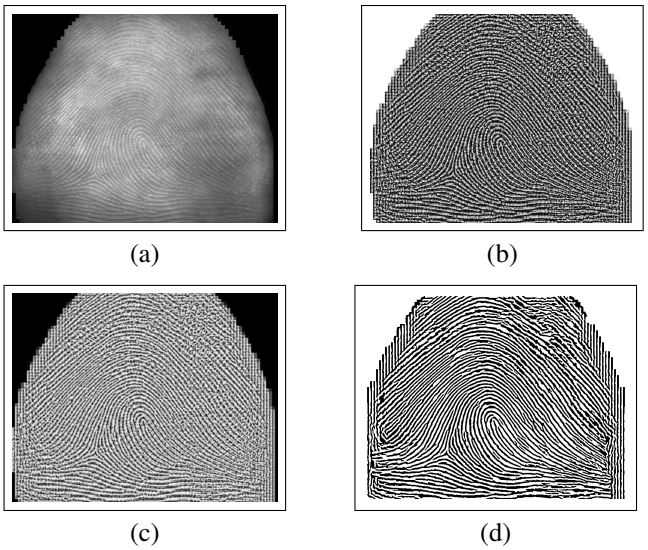

Fig. 3. Initial processing steps: (a) original image, I (712×560 *pixels*, 8 bits per pixels); (b) image after equalization and gamma transformation, $I_{h\gamma}$; (c) filtered image I_{f1} with $h1 = 3$; and (d) I_{b1} binarized image after *mindtct* is applied to I_{f1}. The images I_{fi} and I_{bi}, for $i = 2..4$, are not shown.

Images of 100 different fingers compose the test set. Given the fact that two acquisitions of each finger were performed, a total of 200 fingerprint images were generated. All fingerprints were processed by the algorithm described in Section 2. After that, a quality score using NFIQ (NIST – National Institute of Standards and Technology – Fingerprint Image Quality) software was calculated for each fingerprint. NFIQ uses a classifier based on artificial neural networks that returns an integer number from 1 to 5, which mean: 1 (excellent); 2 (very good); 3 (good); 4 (fair); and 5 (poor). Details about how this score is generated can be found in the document published by Tabassi and collaborators [11]. Roughly speaking, the software is based on: (a) quality maps that integrate informations about contrast, ridge flow and curvatures; (b) fingerprint area; (c) total number of minutiae; and (d) number of minutiae per specific quality thresholds. The quality of a minutiae is estimated based on two factors: (i) its position on the quality map; and (ii) the mean and standard deviation of the pixels of its immediate neighborhood. Figure 5(a) shows the results generated by NFIQ for our test set. Approximately 90% of fingerprints are classified as good, very good or excellent.

In a second experiment, processed fingerprints were sub-

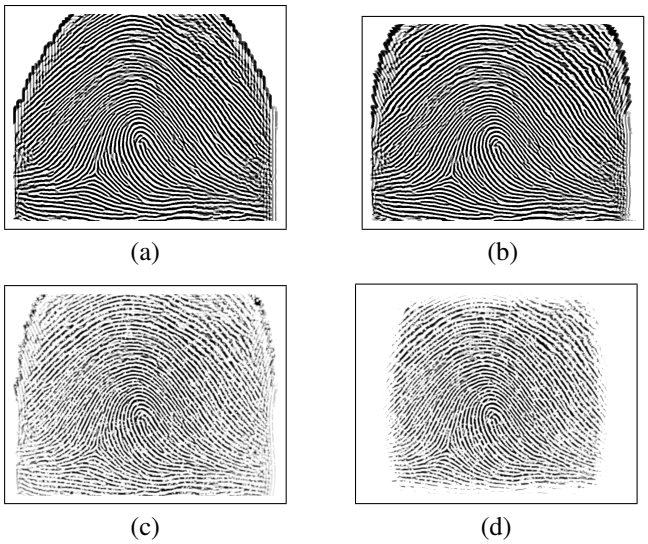

Fig. 4. Final processing steps: (a) I_M (average image calculated from I_{bi} images); (b) I_D, resulting image after geometrical correction applied to I_M (each line of the image is extrapolated in both directions in order to fit the estimated polynomials); (c) I_T, resulting image after synthetic texture is applied to I_D; and (d) I_F, final image after cropping and fading of I_T.

mitted to *bozorth3* [9], the fingerprint matching software from NIST. The objective was to evaluate how a traditional touchbased fingerprint matcher would perform on our processed images. In order to evaluate matching performance, false rejection and false acceptance rates are calculated for different *bozorth3* thresholds and then the EER (equal error rate) is determined. To calculate false rejection rate, one of the two images from each of the 100 fingers is matched against the other sample of the same finger, totaling 100 comparisons. The false acceptance rate is calculated by matching the two images from each finger against both images from all other fingers. In summary, two images of finger 1 are matched against all samples of fingers 2 to 100; next, both images of finger 2 are matched against all fingerprints from fingers 3 to 100; and so forth until the 2 images of finger 99 are matched against fingerprints from finger 100, totaling 19800 comparisons.

Finally, one should observe that a matching condition is determined by a similarity score returned by *bozorth3*. Figure 5(b) shows the curves of false acceptance and false rejection for similarity thresholds varying from 0 to 150. The observed EER is around 4% for a threshold of 14.

4. CONCLUSIONS

In this work, a method to enable the compatibility between touchless and touchbased biometric fingerprinting systems was proposed. First, 200 finger samples were acquired using a scanner that does not require any kind of contact. These images went through two main processing steps. The first one,

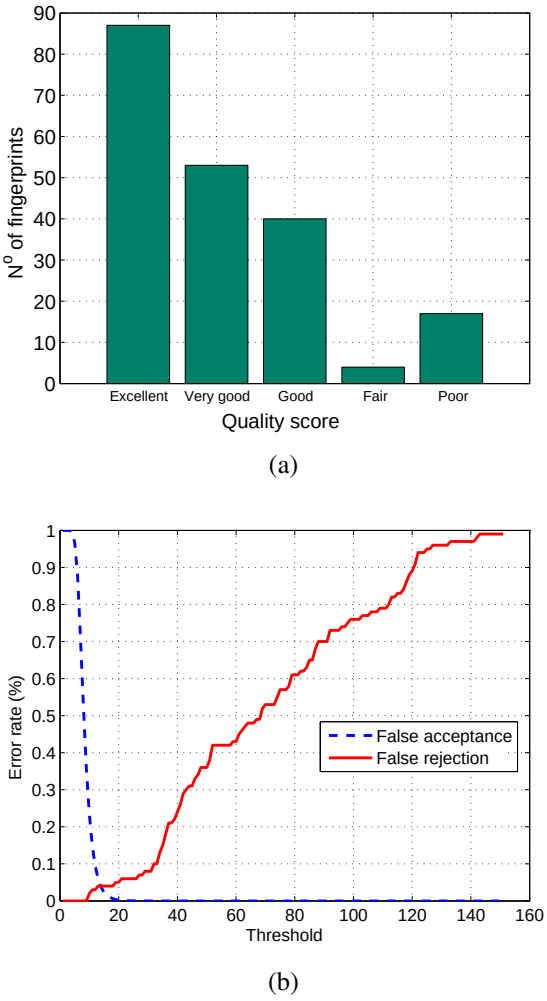

Fig. 5. Results: (a) NFIQ quality scores for 200 test set images: 90% are classified as good, very good or excellent; and (b) false acceptance and false rejection rates are calculated using the *bozorth3* fingerprint matching software. Equal error rate is about 4%.

which reproduces the texture of traditional touchbased fingerprints; and the second one, which approximates the geometric aspect of the nail-to-nail touchbased acquisition process. Two test scenarios were proposed: (a) one to evaluate the quality of processed images using a touchbased quality assessment software; and (b) one to compute matching performance using a touchbased matcher. It is shown that approximately 90% of fingerprint images were classified as good, very good or excellent by NFIQ, the NIST quality estimator used in the scenario (a). Regarding test scenario (b), the EER achieved was about 4%. The initial hypothesis was that touchbased systems may operate transparently with touchless images as long as they are properly processed. The experimental results confirm our hypothesis, showing the viability of the proposed method.

5. REFERENCES

[1] J. Wayman, "A definition of biometrics," in *National Biometric Test Center Colected Works 1997-2000*. San Jose State University, 2000.

[2] R. Allen, P. Sankar, and S. Prabhakar, "Fingerprint identification technology," in *Biometric Systems: Technology, Design and Performance Evaluation*, J. Wayman, A. Jain, D. Maltoni, and D. Maio, Eds., chapter 2. Springer, London, 2005.

[3] R.D. Labati, V. Piuri, and F. Scotti, "Neural-based quality measurement of fingerprint images in contactless biometric systems," in *Neural Networks (IJCNN), The 2010 International Joint Conference on*, july 2010, pp. 1 –8.

[4] Ruggero Donida Labati, Vincenzo Piuri, and Fabio Scotti, "A neural-based minutiae pair identification method for touch-less fingerprint images," in *Computational Intelligence in Biometrics and Identity Management (CIBIM), 2011 IEEE Workshop on*, april 2011, pp. 96 –102.

[5] A. Genovese, E. Muñoz, V. Piuri, F. Scotti, and G. Sforza, "Towards touchless pore fingerprint biometrics: A neural approach," in *2016 IEEE Congress on Evolutionary Computation (CEC)*, July 2016, pp. 4265–4272.

[6] R. Donida Labati, A. Genovese, V. Piuri, and F. Scotti, "Toward unconstrained fingerprint recognition: A fully touchless 3-d system based on two views on the move," *IEEE Transactions on Systems, Man, and Cybernetics: Systems*, vol. 46, no. 2, pp. 202–219, Feb. 2016.

[7] G. Parziale, "Touchless fingerprinting technology," in *Advances in Biometrics: Sensors, Algorithms and Systems*, Nalini K. Ratha and Venu Govindaraju, Eds., chapter 2. Springer, London, 2008.

[8] D.L. Milgram, "Computer methods for creating photomosaics," *IEEE Transactions on Computers*, vol. C-24, no. 11, pp. 1113–1119, Nov. 1975.

[9] C. Watson, M. Garris, E. Tabassi, C. Wilson, R. M. McCabe amd S. Janet, and K. Ko, *User's Guide to NIST Biometric Image Software*, NIST, 2008.

[10] R. Cappelli, A. Erol, D. Maio, and D. Maltoni, "Synthetic fingerprint-image generation," in *Pattern Recognition, 2000. Proceedings. 15th International Conference on*, 2000, vol. 3, pp. 471–474 vol.3.

[11] E. Tabassi, C. L. Wilson, and C. I. Watson, *Fingerprint Image Quality*, NIST, 2004.